

A Study on Structural Safety of Concrete Arch Dams During Construction and Operation Phases

Mohammad Alembagheri 

Received: 14 May 2018 / Accepted: 10 July 2018 / Published online: 11 July 2018
© Springer Nature Switzerland AG 2018

Abstract A methodology is proposed for static safety evaluation of concrete arch dams during their construction and operation phases. It includes foundation modeling, stage-construction process, thermal post-cooling analysis, realistic behavior of contraction and peripheral joints, reservoir filling, and operational thermal loading. The structural stability and safety is assessed using safety indices. The proposed methodology is applied to a typical concrete arch dam. The dam is three-dimensionally modeled along with its foundation using finite element method. Different foundation properties are investigated in homogeneous and inhomogeneous conditions including distinct soft rock layers. The stability and safety of the dam-foundation system is evaluated through some analysis cases, which show the importance of various features presented in the model.

Keywords Concrete arch dams · Safety evaluation · Stage-construction · Post-cooling · Contraction and peripheral joints · Inhomogeneous foundation

1 Introduction

High concrete arch dams are among most important huge infrastructures. Their failure causes catastrophic consequences, so their safety evaluation is of great importance. They are located in rock canyons, curved upstream in plan, and have two distinct behaviors under applied forces: arch and cantilever actions. The dam-foundation interface represents a discontinuity extending across the entire cross section, which is named peripheral joint between the dam and the rock foundation (FERC 1999). The arch dams consist of several concrete blocks called monoliths. The monoliths are separated through vertical contraction joints. They are constructed individually, and the contraction joints are grouted step-by-step after that the monoliths are erected up to specific heights (Sevim et al. 2014). Before joint grouting, the monoliths mainly behave under the cantilever action, but after grouting, they are integrated and the arch action initiates. This specific construction process, which is called stage construction, changes the stress distribution within the dam and its abutments (USACE 1994). If the dead load is applied to the dam model all at once, without taking into account the construction process, fictitious stresses will be indicated (Federal Energy Regulatory Commission 1999). The stage construction may result in decreasing the maximum tensile stress and changing its location (FREC 1999; Pourbakhshian and Ghaemian 2015; Hosseinzadeh et al. 2013;

M. Alembagheri (✉)
Department of Civil and Environmental Engineering,
Faculty of Civil and Environmental Engineering, Tarbiat
Modares University, Tehran, Iran
e-mail: alembagheri@modares.ac.ir

Takaloozadeh and Ghaemian 2014). A number of studies have been also conducted to investigate the effects of peripheral and contraction joints in the analysis of arch dams (Azmi and Paultre 2002; Sevim et al. 2011a, b; Zou et al. 2017; Bayraktar et al. 2009; Yazdani and Alembagheri 2017; Sevim et al. 2012; Du et al. 2007; Du and Jin 2007).

Narrow canyons with steep walls of stable rock are most suitable places for concrete arch dams (USACE 1994). Abutment stability of arch dams is very important and must be controlled during their analysis and design (Takaloozadeh and Ghaemian 2014). Typically, massive rock foundations are inhomogeneous and include various kinds of discontinuities (Chen et al. 2012). The geological conditions of dam-sites are complicated and determined by the geometry of their structure and the properties of the rocks and discontinuities (Hosseinzadeh et al. 2013). Usually, the major discontinuities, such as single large joints or faults, can be taken into account for mechanical analysis. Consideration of the effect of small discontinuities may be included using the continuous modeling (Chen et al. 2008, 2012). The mechanical parameters of the rock masses are the basic input for analysis of dam-foundation systems, which can considerably affect their response (Pausz et al. 2016; Joshi et al. 2015; Alonso et al. 2014; Lin et al. 2007; Zhang et al. 2008).

During construction of an arch dam, concrete would be placed in large quantities. The exothermic cement hydration, low conductivity of concrete, evolutionary dam construction process and environmental conditions result in a different temporal and spatial temperature evolution within mass concrete which leads to according differential volume changes of concrete (Gaspar et al. 2014; Sheibany and Ghaemian 2006; Noorzaei et al. 2006; Jaafar et al. 2007). Thus, thermal stresses could be generated, and when they exceed the current tensile strength of concrete, thermal cracking may be observed. Therefore, this kind of structures should be constructed paying attention to the generation of thermal cracks to make sure of its safety and serviceability. Various thermal schemes, for example in the form of pre- and post-cooling techniques, are required to prevent undesirable cracking (Federal Energy Regulatory Commission 1999; USACE 1994).

Damages of arch dams and their abutments have been frequently observed during construction, first

reservoir filling or early years of operation before that any extreme loading like earthquake occur; for example Zerveila and Zeuzier dams in Switzerland (SNCLD 1985), Daniel Johnson dam in Canada (Florin 2013), Xiaowan and Jinping dams in China (Wang et al. 2011), Koln Brein dam in Austria (Lombardi 1991), El Atazar dam in Spain (Urbistondo and Yges 1985), and Karun 4 dam in Iran (Obernhuber 2015). It shows the importance of proper analysis and design of arch dams under the most prominent static loads, i.e. self-weight, hydrostatic pressure, and thermal loads. If an arch dam is appropriately designed for static loads, it can presumably survive the dynamic loads (Federal Energy Regulatory Commission 1999). Moreover, any model to be used for earthquake analysis of arch dams should properly represent the actual behavior of dam under static loads caused by construction and operation period. Therefore, robust analysis of arch dams under static loads is of great importance in their structural design, and the need for accurate modeling of concrete arch dams is still being felt.

In this paper, the static behavior of a typical concrete arch dam during its construction and operation is assessed using a proposed computational methodology. The proposed methodology contains main features like stage construction, post-cooling, realistic behavior of the joints, reservoir filling, and operational thermal loading. The dam is three-dimensionally modeled along with its foundation using finite element method. Different foundation properties are investigated in homogeneous and inhomogeneous conditions including distinct soft rock layers. The stability and safety of the dam-foundation system is evaluated through some analysis cases which show the importance of various features presented in the model.

2 Numerical Procedure

This section outlines the governing equations, boundary conditions, constitutive behaviors and numerical modeling of the main features of the model, and describes safety evaluation indices and the proposed computational methodology.

2.1 Heat Transfer and Stress/Displacement Analysis

In large arch dams, the concrete temperature rising from the hydration of cement, coupled with the low conductivity of concrete can induce high thermal gradient in the interior mass and exterior surface of the dam. During cooling process of the dam, due to the presence of interior and external restraints such as foundation restraint, this thermal gradient can cause significant thermal stresses. Therefore, the thermal analysis of arch dams considering real construction schedule plays an important role in their design and construction (Jaafar et al. 2007). The temperature effects on arch dams can be studied in two distinct phases: (1) construction, in which the main heat source and sink are hydration of concrete and artificial pipe cooling (post-cooling), respectively (Sheibany and Ghaemian 2006); and (2) operation, in which the dam is subjected to the environmental action like ambient and reservoir temperature variations (Noorzaei et al. 2006). The results of the heat transfer analysis can be used for thermal stress analysis.

The transient heat conduction equation for a homogenous and isotropic material, whose thermal conductivity is independent of temperature, is defined in the 3D Cartesian space as (Leger et al. 1993):

$$\frac{\partial^2 T}{\partial x^2} + \frac{\partial^2 T}{\partial y^2} + \frac{\partial^2 T}{\partial z^2} = \frac{\rho \cdot c}{k} \frac{\partial T}{\partial t} - \frac{Q}{k} \tag{1}$$

where ρ is the density, in kg/m^3 ; c is the specific heat, in $\text{J}/(\text{kg K})$; T is the temperature, in K ; t is the time, in seconds; k is the isotropic thermal conductivity coefficient, in $\text{W}/(\text{m K})$; Q is the internal heat source per unit volume (e.g. due to hydration), in W/m^3 ; and x, y, z are the Cartesian coordinates. In the steady-state heat conduction, the first term in the right hand side of Eq. (1) will be omitted. The boundary conditions are

$$T = T_p \quad \text{on } \Lambda_p \tag{2a}$$

$$k \frac{\partial T}{\partial n} = q_n \quad \text{on } \Lambda_s \tag{2b}$$

where T_p is the prescribed temperature, and q_n is the heat flux in the outflow normal direction (n) of Λ_s , in W/m^2 . In arch dams, the maximum hydration temperature and the grouting temperature are usually controlled within the dam body using the post-cooling techniques, so they could be considered as prescribed

temperatures. At the dam-air interface, the heat flux being transferred between the dam and the surrounding air on Λ_s is indicated as convection, and is given by Newton’s law of cooling:

$$q_n = h(T - T_A) \tag{3}$$

where h is the convection coefficient, in $\text{W}/\text{m}^2 \text{K}$; T is the temperature of the dam and T_A is the ambient temperature. If a large convection coefficient is used, for example $h = 10^{10}$, the surface temperature will follow the air temperature exactly (Polivka and Wilson 1976). Other sources of heat flux like radiative heat transfer or solar radiation are not considered in this research. At the dam-water interface, there will be a small error by assuming that the concrete temperature is equal to the water temperature. This is because of small thermal gradient at this interface (Leger et al. 1993). Thus, no convection is assumed to occur at this boundary.

Using the finite element method, the temperature T is expanded over an element by:

$$T(t) = [N]^T \{T(t)\}^e \tag{4}$$

where $[N]^T$ is a matrix containing the shape functions and $\{T\}^e$ is the vector of nodal unknown temperatures. Using the Galerkin weighted residual approach, the system matrix equation for heat flow equilibrium can be derived as (Cook 2007):

$$[A]\{\dot{T}(t)\} + [B]\{T(t)\} = \{Q(t)\} \tag{5}$$

in which $[A]$ is the system heat capacity matrix, $[B]$ is the system thermal conductivity matrix, and $\{Q(t)\}$ is the system heat flux vector. In the presence of convection, they are defined as:

$$[A] = \sum_{elements} \int_{\Omega_e} \frac{\rho \cdot c}{k} [N][N]^T d\Omega \tag{6a}$$

$$[B] = \sum_{elements} \int_{\Omega_e} \left(\frac{\partial [N] \partial [N]^T}{\partial x^2} + \frac{\partial [N] \partial [N]^T}{\partial y^2} + \frac{\partial [N] \partial [N]^T}{\partial z^2} \right) d\Omega + \int_{\Gamma_e} [\hat{N}] \frac{h}{k} d\Gamma \tag{6b}$$

$$\{Q(t)\} = \sum_{elements} \int_{\Omega_e} [N] \frac{Q}{k} d\Omega - \int_{\Gamma_e} [\hat{N}] \frac{h}{k} T_F d\Gamma \tag{6c}$$

where Ω and Γ represents the domain and surface of elements, Σ represents the common assembly process through various elements, and the sign \wedge indicates the restriction of the shape functions to an element face (Sheibany and Ghaemian 2006). The system of heat transfer equations is valid over the dam-foundation domain. In the absence of any radiation, $\{Q(t)\}$ and $[B]$ can be formulated independent of the unknown temperatures. This equation system can be solved directly by a step-by-step integration procedure.

Considering the balance of forces, the relationship between the nodal displacement vector, $\{U\}$, and the force vector $\{F\}$ generated by the body and surface forces in addition to the difference between obtained nodal temperatures, $\{T\}$, and nodal closure temperatures, $\{T_0\}$, can be presented in the following manner:

$$[K]\{U\} = \{F\} \quad (7)$$

$$[K] = \sum_{elements} \int_{\Omega_e} [B]^T [D] [B] d\Omega \quad (8a)$$

$$\{F\} = \{F_B\} + \{F_S\} + \sum_{elements} \int_{\Omega_e} [B]^T [D] \{\varepsilon_{th}\} d\Omega \quad (8b)$$

$$\{\varepsilon_{th}\} = \alpha(\{T\} - \{T_0\}) \quad (8c)$$

where $[K]$ is the stiffness matrix, $[D]$ is the stress–strain matrix, $[B]$ is the strain–displacement matrix, $\{F_B\}$ and $\{F_S\}$ are the body and surface force vectors, respectively, $\{\varepsilon_{th}\}$ is the thermal strain vector, and α is the coefficient of thermal expansion.

2.2 Joints Constitutive Model

As it was stated, arch dams are not monolithic structures, and have discontinuities such as peripheral and vertical contraction joints. These joints represent planes of weakness when they are subjected to tensile and/or shear stresses. Linear analysis without considering the joint effects engenders tensile stresses that are greater than joints can withstand (Azmi and Paultre 2002).

In this paper, the joints are modeled using 3D nonlinear cohesive contact definition that allows joint opening and closing as well as tangential displacement. As it is shown in Fig. 1, the relative displacement between two adjacent surfaces of the joint have

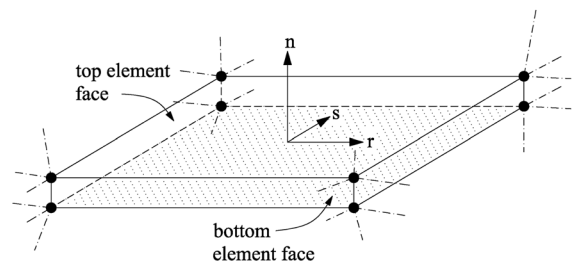


Fig. 1 Contact between two elements faces and the local coordinates

three components in local coordinate, $\{\delta\} = \{\delta_n, \delta_r, \delta_s\}^T$, in which δ_n is the normal displacement, and the tangential displacement could be defined as $\delta_t = \sqrt{\delta_r^2 + \delta_s^2}$. The resisting stresses across the joint are nonlinear functions of $\{\delta\}$ and depend on the state of the joint: open or closed (Azmi and Paultre 2002). The joint constitutive behavior is illustrated in Fig. 2. When the normal stress across the joint, σ , is positive, then it experiences tension in normal direction. In this situation, the tangential stresses are zero, while the normal tensile stress can be transferred up to tensile strength of the joint, σ_u . The normal tensile stiffness of the joint perpendicular to the joint is indicated as K_n . Beyond the σ_u , the stress softening would occur until $\delta_n = \delta_{n0}$, after which the normal stress would be zero.

When the joint is in compression, $\sigma < 0$, it is closed, and the normal compressive stress is nonlinear penalty function of the joint clearance, δ_n . It is defined by parameters σ_{n0} and δ_{n0} (Fig. 2). The tangential displacement of the joint is governed by the Mohr–Coulomb friction criterion. The shear strength of the joint, τ_u , is defined as:

$$\tau_u = \min(\tau_{crit}, \tau_m) \quad (9)$$

$$\tau_{crit} = |\sigma| \cdot \tan \varphi; \quad \tau_m = n \cdot \sigma_y / \sqrt{3} \quad (10)$$

where τ_{crit} is the sliding threshold of the joint, φ is the Mohr–Coulomb friction coefficient, τ_m is the maximum shear strength of material in contact; it arises due to the presence of shear keys across the contraction joints, σ_y is the uniaxial compressive yield stress of the material, and n measures the surface ratio covered by the shear keys to the total area of contraction joint. When the joint is closed, the tangential stress is elastic with stiffness K_t in both directions r and s only if the resultant of the tangential stresses, $\tau_t = \sqrt{\tau_r^2 + \tau_s^2}$, is

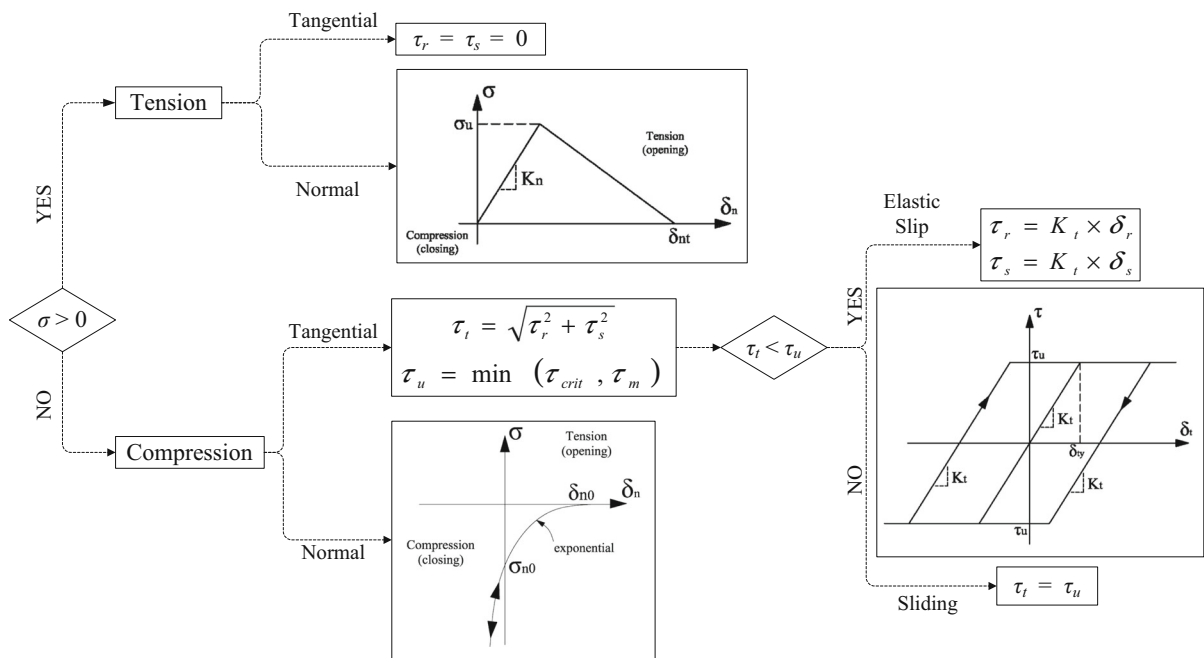


Fig. 2 Joints constitutive behavior

less than the shear strength, τ_u . Here the elastic slip would occur up to $\delta_t = \delta_{ty}$. When the tangential stress reaches the value of the shear strength, sliding occurs in the direction of t while the stiffness remains the same K_t in the tangential direction (Azmi and Paultre 2002).

2.3 Safety Evaluation

The safety evaluation of arch dams is a complex problem because of the uncertainties related to the prediction of the spatial and temporal variations of applied loadings (Federal Energy Regulatory Commission 1999). Temperature variation and the associated thermal stresses must be evaluated to define a defensive measure in dam safety analysis, which may contain designing distance of adjacent monolith joints, and determining optimized grout temperature (Sheibany and Ghaemian 2006). Before investigating the seismic safety of arch dams, it is essential to quantify their static safety that exists at the time the earthquake occurs, which may vary significantly from winter to summer conditions (Leger et al. 1993). In most cases, linear analysis along with engineering judgment is sufficient for stability analysis and safety evaluation of arch dams (USACE 1994). The stress safety of the

dam body can be controlled using simple safety factors:

$$SF_i = \frac{f_i}{s_i}, \quad i = t \text{ or } c \tag{11}$$

where f is the uniaxial strength, s is the principal stress, and subscripts t and c represent tension and compression, respectively. These safety factors can be checked with their allowable values as recommended by Federal Energy Regulatory Commission (1999). The SF_t can represent the cracking index of the dam body. In addition, the biaxial failure curve of concrete can be utilized for more accurate safety control. It can be produced using the modified relationships represented by Kupfer et al. (1969).

Thrust forces of arch dams could cause significant stresses in their rock foundation. The stress safety could be evaluated, in the same way as the dam body, for the foundation and the abutments. Another safety check could be conducted on the joints status. The relative position of the dam and the foundation would be controlled by the peripheral joint status. The joint opening, especially on the upstream side during reservoir filling, would allow the water to penetrate inside the joints and endanger the dam safety. The relative joint sliding could destroy the water-stops and

drainage pipes within the dam body and between the dam and the foundation.

2.4 Proposed Computational Methodology

Arch dams are constructed in sequences called stage construction. The stage construction can be modeled using the “odd and even” analysis or the “birth and death” technique in several stages (USACE 1994). It is carried out using two separate sub-stage analyses and superimposing their stress results. In the first sub-stage analysis, normal stiffness and dead weight for odd cantilevers are considered, while even cantilevers’ stiffness and weight density are reduced to zero. This process is vice versa with respect to odd and even cantilevers’ properties for the second dead weight analysis (Hosseinzadeh et al. 2013). This is an approximate procedure. Since the entire model is present during the analysis, undesirable deformation occurs for monoliths, however, the next stage is constructed on deformed position of the previous stage. Also, this method along with real modeling of peripheral and contraction joints may result in convergence problems, so different approach is selected for modeling the stage construction.

The methodology and the computational algorithm, which will be used in this study, is illustrated in Fig. 3. It includes five general sections: (a) model definition, (b) foundation analysis, (c) stage construction, (d) operation analysis, and (e) safety evaluation. The construction stages are modeled with actual separation of odd and even cantilevers through contraction joints. A deactivate-activate procedure, summarized as follows, is adopted to actually simulate the construction sequence. The dam body is divided into several horizontal layers. After defining the basic properties of the model, all components of the model, i.e. the foundation and the dam layers, are deactivated. First, the foundation, which may be inhomogeneous, is activated before construction of the dam. The activation process means assembling the system matrices and incorporating the boundary conditions of undeformed shape. The weight of the foundation rock is applied without the presence of the dam, and the resulted stresses are saved and defined as initial stress situation for the undeformed foundation in the next step. So the dam is exactly located in prescribed position on the foundation. If foundation rock weight is applied without removing the dam body, large

stresses are generated in the dam that significantly affect the precision of the analysis. After that, the dam is activated stage-by-stage. In each stage of dam construction, say stage i : (1) the foundation and all previous added dam construction stages are activated, and the stress results from the analysis of previous stage are inputted as initial stress state for the undeformed position of the system before adding new dam layer; (2) the new dam layer along with its contraction joints activated just in normal direction, and peripheral joint in contact with foundation activated in both normal and tangential directions are augmented; (3) the tangential behavior of contraction joints between the monoliths of the last previous stage, i.e. stage $(i - 1)$, is activated which means the grouting of the previous stage; (4) the system is analyzed under self-weight of the new dam stage and its thermal loading resulted from the post-cooling; (5) the obtained stresses are saved as initial stresses for the next step. The post-cooling process includes steady-state thermal analysis from the hydration temperature to the grouting temperature. Both temperatures are assumed uniform throughout the dam layers. This procedure will be continued until completion of the dam construction. In this way, the initial dam shape before operational loading is maintained, and the extra arching effect, which is expected to occur in monolithic modeling, decreases and the resultant stresses are much closer to real values. After the dam is completely constructed, the resulted stresses are assigned to the undeformed position of the system before applying the hydrostatic pressure of reservoir, and the ambient temperature. Then the system is analyzed under the operational loadings. The superimposing procedure cannot be straightforwardly used because of joint nonlinearities. In real projects, the joints grouting may be totally checked before reservoir filling, so they are in initial undamaged state before dam operation. In addition, the dam displacements during operation are of great importance; they may be measured using the pendulum instruments which are installed within the dam body after its completion (USACE 1994). The safety of the system can be evaluated during the stage construction, after the dam completion, and after application of the external loads.

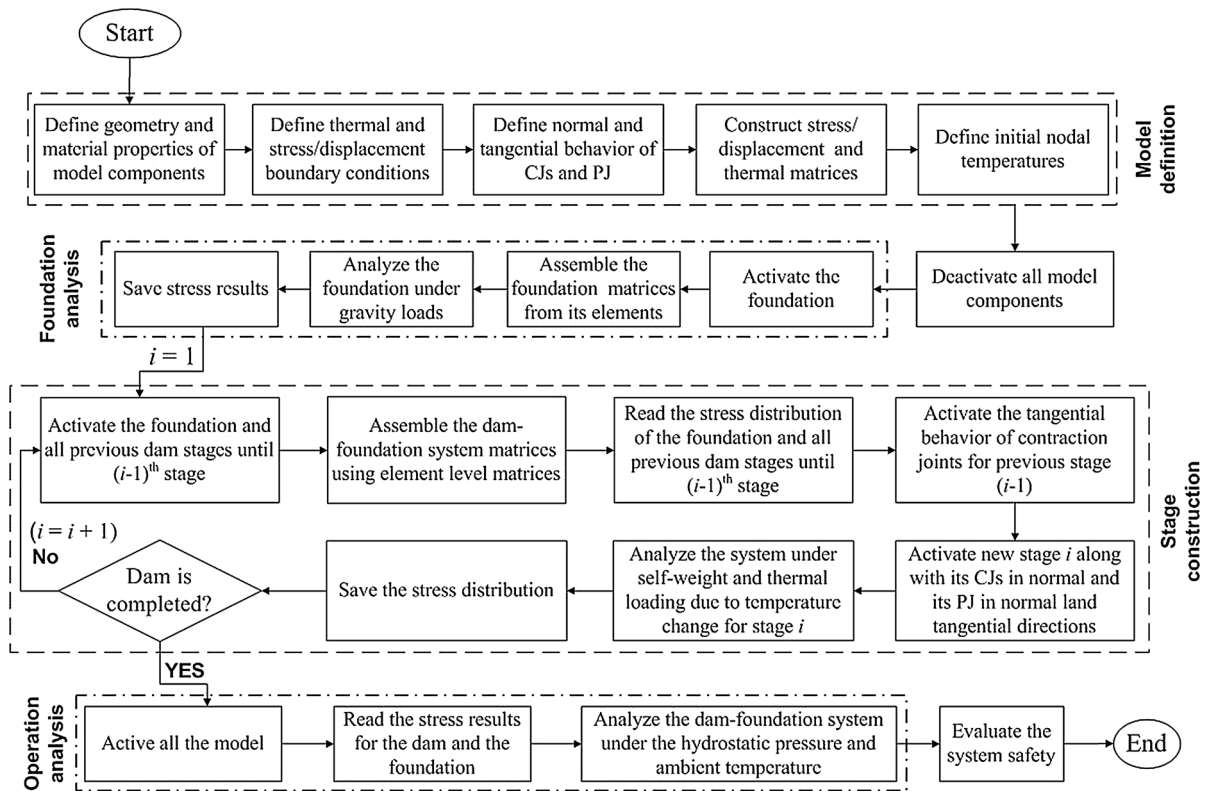


Fig. 3 Flowchart of the proposed methodology; *i* measures the number of construction stages. *CJ* contraction joints, *PJ* peripheral joint

3 Description of Case Study

The proposed methodology is applied to a typical arch dam with layout like Morrow Point dam. It is 142 m high arch dam with the crest length of 280 m. Its thickness varies from 15.74 m at the base to 3.66 m at the crest. The dam is divided into 16 monoliths using 15 contraction joints, as shown in Fig. 4a; a peripheral joint is considered at the dam-foundation interface. The assumed properties for the contraction and peripheral joints, as described in Sect. 2.2, are listed in Table 1. The normal tensile strength is considered just for the peripheral joint due to cohesion between the concrete and the rock. It is assumed that the shear keys cover 60% area of the contraction joints, so $n = 0.6$ in Eq. (10) for calculating the maximum shear strength of concrete. Also in this equation, σ_y is considered to be 30 MPa. The joint tangential stiffness, K_t , is computed in each instant using τ_u and δ_{ty} .

Because the maximum height of each monolith grouting is typically limited to 30 m (Takaloozadeh and Ghaemian 2014), the dam construction process is

modeled in 5 stages (layers) as shown in Fig. 4b. The post-cooling thermal analysis for each dam stage is conducted after arriving to its hydration temperature, which is assumed to be 27 °C, then reducing the dam layer’s temperature from the hydration temperature to the post-cooling or grouting temperature, which is assumed to be 17 °C. Since the dam concrete is approximately free to deform when the concrete is placed, the thermal analysis during the cement hydration is not conducted, and the hydration temperature is considered as zero-stress temperature. The hydration and post-cooling temperatures are assumed to be uniform throughout the dam layer. The effects of latent heat during phase change are not taken into consideration. Therefore, the mechanical and thermal properties of concrete are assumed to be constant, isotropic, and temperature independent.

During the operation, the unusual loading combination is the dead load + hydrostatic pressure of maximum water level + ambient temperature in both summer and winter (Federal Energy Regulatory Commission 1999). The maximum water level is

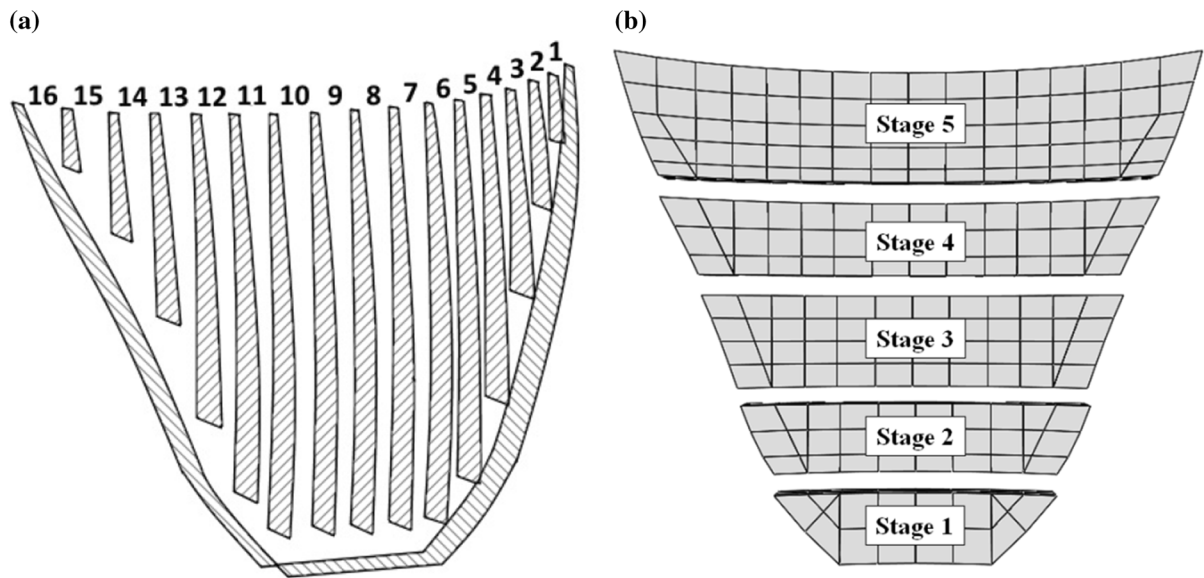


Fig. 4 **a** The dam body and its monoliths and joints, **b** layers considered for the five-stage construction

Table 1 Joints properties used in this research

Property	Normal direction					Tangential direction	
	Joint in tension			Joint in compression		φ	δ_{ry} (mm)
	K_n (GPa/m)	σ_u (MPa)	δ_{nt} (mm)	δ_{no} (mm)	σ_{no} (MPa)		
Contraction joint	20	0.0	–	0.1	1	50°	2
Peripheral joint	20	1.5	10	0.1	1	60°	2

considered at the dam crest level, which means full reservoir. It has been shown that the uplift pressures are not much important in the analysis of arch dams (Federal Energy Regulatory Commission 1999), so they are not considered in this research. Proper and coordinated climatic conditions are assumed in the thermal analysis. Because of small thickness of the dam body adjacent to ground in comparison with other interfaces, foundation rock effect on temperature distribution is not considered. The mean annual, summer, and winter ambient air temperature is assumed 20, 34, and 13 °C, respectively. The effect of solar radiation is taken into account by increasing the ambient summer and winter temperatures by 2 and 5 °C, respectively, to account for the solar radiation heating of the concrete surface (USBR 1997). At the dam-air interface, the boundary condition is convection between concrete surface and surrounding air.

The convection coefficient, h , is applied to the downstream (DS) surface (Jaafar et al. 2007). At the upstream (US) surface, it is assumed that the concrete temperature in contact with water is equal to the water temperature. The water temperature distribution depends on the geometry of the reservoir and the environmental condition acting at its surface such as air temperature. In this study, Bofang method (1997) is utilized to predict the water temperature stratification along the depth of the full reservoir at summer and winter as shown in Fig. 5.

The dam is three-dimensionally modeled along with its foundation using 8-node linear solid finite elements. However, due to the presence of the joints, some wedge elements are unavoidable, but it is attempted to distance them from the dam-foundation interface, which is a critical region (Fig. 7a). Three element layers are assigned along the dam thickness.

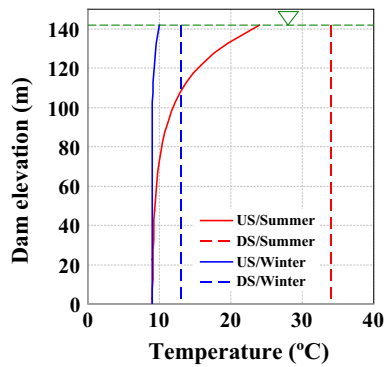


Fig. 5 Water and air temperature distribution considered along the dam height on the upstream (US) and downstream (DS) faces, in summer and winter conditions

The foundation is extended to at least twice the dam height in all directions (Fig. 7b) (Federal Energy Regulatory Commission 1999). The exterior side edges of the foundation are restrained in horizontal direction, but its bottom edge is fixed in all directions.

The dam-foundation system is analyzed using the proposed computational methodology described in Sect. 2.4. Some analysis cases are considered by suppressing some parts of the methodology to show the importance of various model features. The analysis cases are listed in Table 2. In the analysis case 1, all the joint surfaces are tied together so there is no joint sliding and opening. The contraction and peripheral joints are present in the rest of models. In models without stage construction, i.e. the cases 1 and 2, the dam self-weight is applied all at once. In the construction phase, all cases are analyzed under the

self-weight. The post-cooling thermal analysis is also applied just in the cases 4 and 5. In the operation phase, all models are analyzed under the full reservoir hydrostatic pressure; the case 5 is also analyzed under the ambient temperature loading of summer and winter.

All cases are investigated in two different categories: (a) homogeneous foundation, (b) inhomogeneous foundation. In the inhomogeneous foundation, a soft rock layer is inserted within the foundation which is a common geological condition at the dam-sites (Pausz et al. 2016). The inhomogeneous foundation category includes two sub-categories: (1) horizontal soft layer, with dimensions and properties shown in Fig. 6a; and (2) inclined soft layer, shown in Fig. 6b. The dam concrete and the foundation rock are assumed isotropic, linear elastic with the mechanical and thermal properties listed in Table 3. Two distinct mechanical properties are considered for the horizontal soft rock layer: $E_2 = 12$ GPa with $\nu_2 = 0.25$; and $E_2 = 9$ GPa with $\nu_2 = 0.26$. The latter is considered for the inclined soft rock layer. The finite element mesh of the dam body and the homogenous foundation are shown in Fig. 7. Approximately the same mesh density is applied for the inhomogeneous foundation models.

4 Structural Safety Evaluation

In this section, the results of the analysis cases in the homogenous and inhomogeneous foundation

Table 2 Cases analyzed in this research

Analysis case	Model feature			Operational loading combination
	Joints	Stage construction	Post-cooling	
1	X	X	X	S ^a + R ^b
2	✓	X	X	S + R
3	✓	✓	X	S + R
4	✓	✓	✓	S + R
5	✓	✓	✓	S + R + T ^c

Symbol ✓ means presence and symbol X means not-presence of the model feature

^aSelf-weight

^bFull reservoir hydrostatic pressure

^cAmbient temperature loading

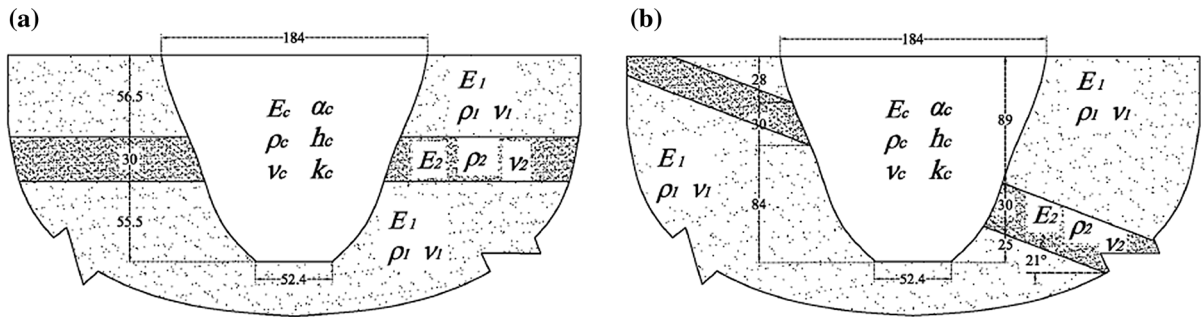


Fig. 6 Inhomogeneous foundation models from upstream view: **a** horizontal soft layer, **b** inclined soft layer. All dimensions are in meters. The foundation is extruded from the shown configuration in stream direction

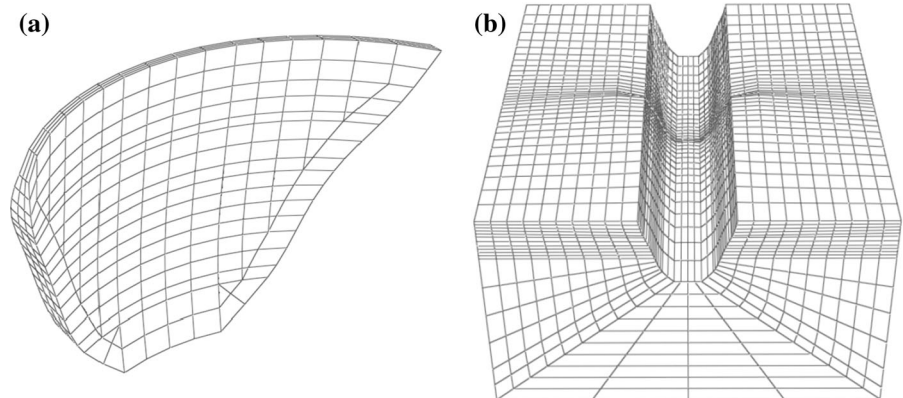
Table 3 Mechanical and thermal properties of the system analyzed

Property	Value		
	Dam concrete	Foundation rock	
		Homogeneous	Inhomogeneous
<i>Mechanical properties</i>			
Young’s modulus (GPa)	$E_c = 24$	$E_1 = E_2 = 18$	$E_1 = 18; E_2 = 12$ and 9
Density (kg/m^3)	$\rho_c = 2483$	$\rho_1 = \rho_2 = 2643$	$\rho_1 = \rho_2 = 2643$
Poisson’s ratio	$\nu_c = 0.2$	$\nu_1 = \nu_2 = 0.22$	$\nu_1 = 0.22; \nu_2 = 0.25$ and 0.26
<i>Thermal properties</i>			
Coefficient of thermal expansion ($10^{-6}/\text{K}$)	$\alpha_c = 10$	–	–
Convection coefficient [$\text{W}/(\text{m}^2 \text{K})$]	$h_c = 23.2^a$	–	–
Thermal conductivity [$\text{W}/(\text{m K})$]	$k_c = 2.62$	–	–

The parameters are shown in Fig. 6

^aFor average annual wind speed of 3.0 m/s

Fig. 7 Finite element mesh of **a** the dam body, and **b** the homogeneous foundation



categories are presented, and the safety of the dam-foundation systems is evaluated.

4.1 Stress Safety Evaluation

The safety of the system is evaluated during the construction and the operation phases. The peak

Table 4 Peak tensile stress, in MPa, for the dam body in various foundation categories

Analysis Case	Load combination	Foundation rock category			
		Homogeneous	Inhomogeneous		
			Horizontal soft layer		Inclined layer
			$E_2 = 12$ GPa	$E_2 = 9$ GPa	
1	S ^a	1.489 (2.015)	1.500 (2.000)	1.493 (2.010)	1.492 (2.010)
	S + R ^b	3.819 (0.785)	4.624 (0.648)	4.685 (0.640)	4.638 (0.647)
2	S	1.046 (2.868)	1.142 (2.627)	1.155 (2.597)	1.165 (2.575)
	S + R	1.320 (2.272)	2.217 (1.353)	3.614 (0.830)	2.215 (1.354)
3	S	1.035 (2.898)	0.997 (3.010)	1.015 (2.956)	1.053 (2.849)
	S + R	1.484 (2.021)	2.307 (1.300)	3.897 (0.769)	2.681 (1.119)
4	S + P ^c	1.063 (2.822)	2.153 (1.393)	2.153 (1.393)	2.152 (1.394)
	S + P+R	1.317 (2.278)	2.838 (1.057)	4.296 (0.698)	3.847 (0.779)
5	S + P+R + T ^d /Wi ^e	1.772 (1.693)	3.120 (0.961)	4.920 (0.610)	4.155 (0.722)
	S + P+R + T/Su ^f	2.163 (1.387)	2.870 (1.045)	3.960 (0.757)	3.225 (0.930)

The numbers in parentheses are the related SF_t

^aSelf-weight

^bFull reservoir pressure

^cPost-cooling

^dAmbient temperature

^eWinter

^fSummer

maximum (tensile) and minimum (compressive) principal stresses of the dam body in various foundation categories are listed in Tables 4 and 5, respectively. The tensile and compressive stresses have positive and negative signs, respectively. The stress safety factors, SF_t and SF_c , computed from Eq. (11), considering typical mass concrete’s uniaxial tensile and compressive strength of 3 and 30 MPa, respectively, are also presented in these tables. The allowable values of stress safety factors for unusual loading combination are 1.0 and 1.5 in tension and compression, respectively (Federal Energy Regulatory Commission 1999). The hydrostatic pressure increases both the tensile and compressive stresses.

The evolution of maximum principal stress within the dam body during the construction phase, with and without the post-cooling, i.e. the cases 3 and 4, for various foundation categories are depicted in Fig. 8. It is observed that the peak tensile stress is continuously increased during the construction process with approximately the same value between various models when the post-cooling is not considered. The post-cooling

generally increases the peak tensile stress of the dam body in each construction stage, specifically if there is soft rock layer within the foundation. The maximum variation is observed for the 2nd and 5th stages with approximately the same intensity for various soft rock layer conditions. Therefore, the soft rock layer in conjunction with the post-cooling thermal loading can significantly change the tensile stress values within the dam body.

From Table 4, if the joint sliding and opening are not allowed (case 1), in all categories the SF_t drops below 1.0 when the hydrostatic pressure is applied, because of excessive tension at the dam-abutment interface. The presence of the joints releases these fictitious tensile stresses. Considering the stage-construction process decreases the peak tensile stress during the construction phase, however it increases the tensile stress during the operation phase. The post-cooling of each stage before erection of the next stage, in the case 4, increases the tensile stresses in both construction and operation phases, specifically for the inhomogeneous foundation category. The ambient

Table 5 Peak compressive stress, in MPa, for the dam body in various foundation categories

Analysis Case	Load combination	Foundation rock category			
		Homogeneous	Inhomogeneous		
			Horizontal soft layer		Inclined layer
			$E_2 = 12$ GPa	$E_2 = 9$ GPa	
1	S ^a	– 2.623 (11.43)	– 2.719 (11.03)	– 2.750 (10.90)	– 2.783 (10.78)
	S + R ^b	– 7.649 (3.922)	– 7.937 (3.779)	– 7.975 (3.761)	– 8.102 (3.702)
2	S	– 5.342 (5.616)	– 5.752 (5.215)	– 5.801 (5.171)	– 6.275 (4.780)
	S + R	– 8.881 (3.377)	– 11.81 (2.540)	– 12.36 (2.430)	– 9.554 (3.140)
3	S	– 6.330 (4.739)	– 6.395 (4.691)	– 6.399 (4.688)	– 6.412 (4.678)
	S + R	– 8.969 (3.344)	– 11.37 (2.638)	– 12.58 (2.385)	– 11.91 (2.519)
4	S + P ^c	– 6.441 (4.657)	– 6.446 (4.654)	– 6.418 (4.674)	– 6.423 (4.671)
	S + P+R	– 8.043 (3.729)	– 13.04 (2.300)	– 15.04 (1.994)	– 15.48 (1.937)
5	S + P+R + T ^d /Wi ^e	– 8.813 (3.404)	– 13.82 (2.171)	– 16.24 (1.847)	– 15.35 (1.954)
	S + P+R + T/Su ^f	– 10.55 (2.843)	– 11.70 (2.564)	– 16.75 (1.791)	– 11.74 (2.555)

The numbers in parentheses are the related SF_r

^aSelf-weight

^bFull reservoir pressure

^cPost-cooling

^dAmbient temperature

^eWinter

^fSummer

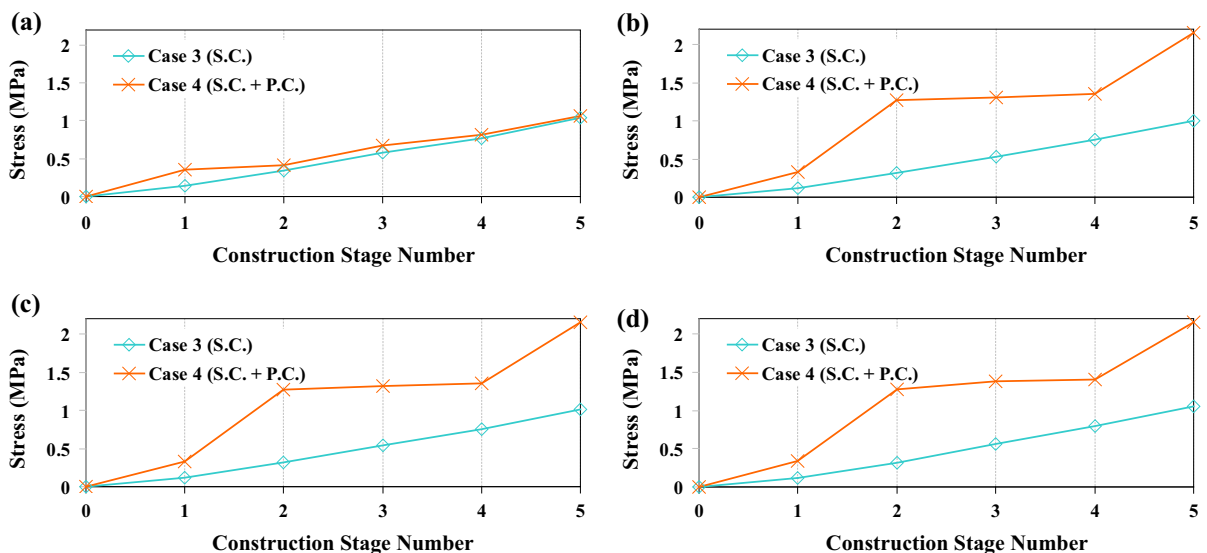


Fig. 8 Evolution of maximum tensile stress in the dam body during the construction phase; *SC* stage construction, *PC* post-cooling. **a** Homogeneous foundation. **b** Inhomogeneous foundation, Horizontal soft layer with $E_2 = 12$ GPa. **c** Inhomogeneous

foundation, Horizontal soft layer with $E_2 = 9$ GPa. **d** Inhomogeneous foundation, Inclined soft layer with $E_2 = 9$ GPa

temperature increases the peak tensile stresses in the homogenous foundation category; the increase is more for the summer conditions, but the SF_t is still higher than the allowable value (1.0). In the inhomogeneous foundation category, the SF_t often drops below 1.0, and, opposite to the homogeneous foundation category, the peak tensile stress is more in the winter than the summer. The horizontal soft layer increases the peak tensile stresses of the dam body in most cases; the softer layer causes more stress. However, inclined soft rock layer with respect to the related horizontal layer, generally causes lower tensile stresses specifically during the operation phase. In all cases of the homogeneous foundation category, except the case 1, the SF_t is always more than 1.0. This is generally the

case for the inhomogeneous foundation category except in the operation phase of the cases 4 and 5. The envelope contours of principal tensile stress of the dam body in the operation phase of the cases 3–5 are shown in Fig. 9. The presence of the soft rock layer causes inhomogeneous displacement of the dam body and changes the tensile stress distribution within the dam body. The tensile stress is more on the downstream face and concentrated near the bottom of soft rock layer. The contour shapes are totally changed during the summer conditions.

In compression, from Table 5, the presence of the joints increases the peak compressive stress of the dam body. Generally, considering both the stage-construction and the post-cooling processes also increases the

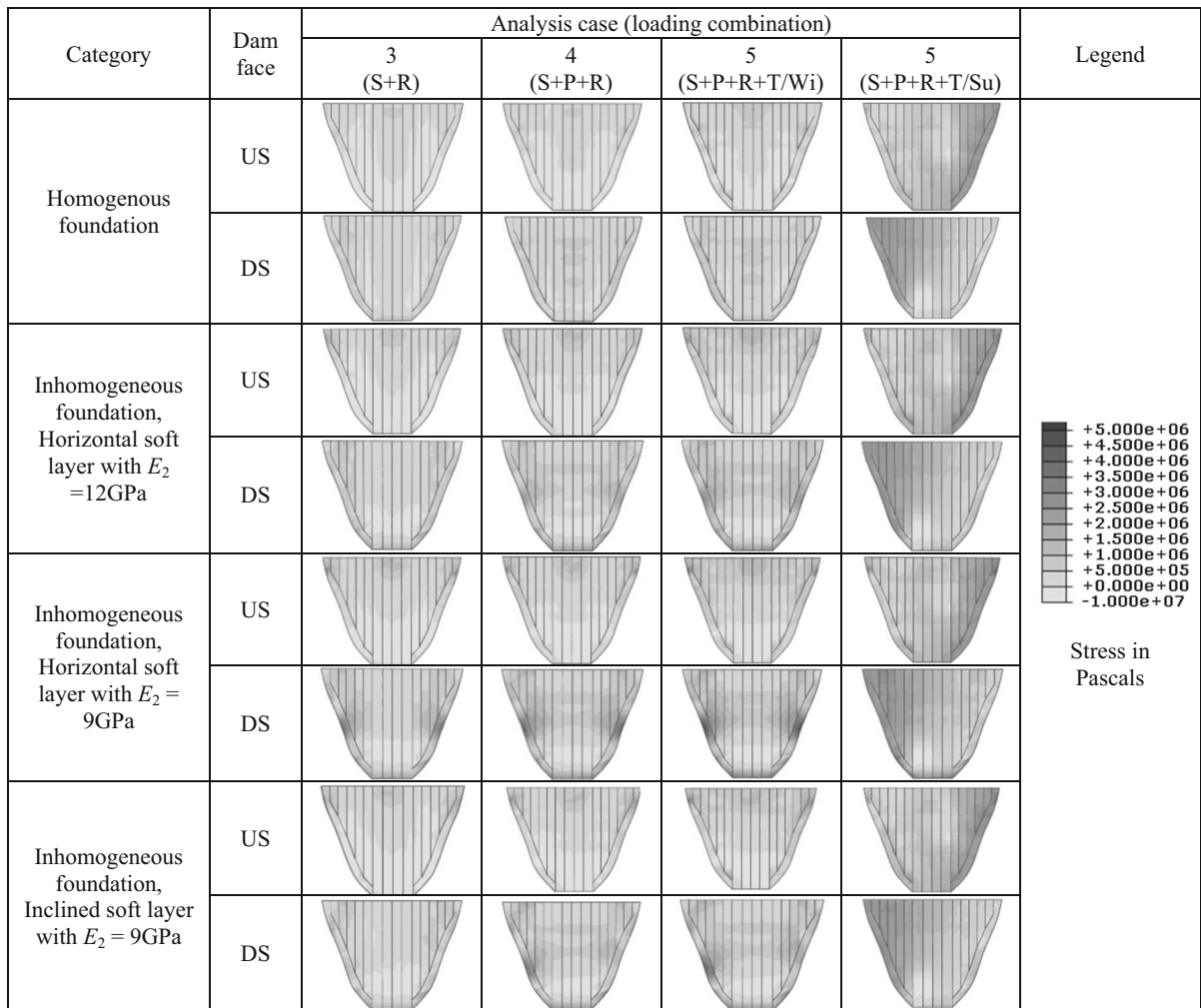


Fig. 9 Envelope contours of principal tensile stress on the upstream (US) and downstream (DS) faces of the dam for the cases 3, 4 and 5 during the operation phase

peak compressive stress in the construction and the operation phases. The ambient winter temperature increases the peak compressive stress in the categories of homogeneous and inhomogeneous foundation with horizontal soft rock layer, however dual changes are observed for the summer condition. The inclined soft rock layer reduces the compressive stress in both summer and winter conditions. In general, the SF_c is higher than the allowable value (1.5) in all cases of various foundation categories. The horizontal soft rock layer increases the peak compressive stress in all cases; the softer layer causes more stress. The inclined soft rock layer, however, in comparison with the related horizontal soft layer, increases the compressive stress during the construction phase, but generally

decreases it during the operation phase. The envelope contours of compressive principal stress of the dam body for the cases 3–5 in the operation phase are shown in Fig. 10. As in the case of tensile stress, the soft rock layer changes the stress distribution of the dam. The peak compressive stress is often concentrated at the bottom of the dam on the downstream face.

The stress safety of the dam body could be more accurately investigated by evaluating the biaxial stress state in which the peak maximum versus the peak minimum principal stress in each nodal point is compared against the biaxial failure curve of concrete. Such a comparison is made in Fig. 11 for the cases 3, 4 and 5 in the operation phase. The biaxial failure curve

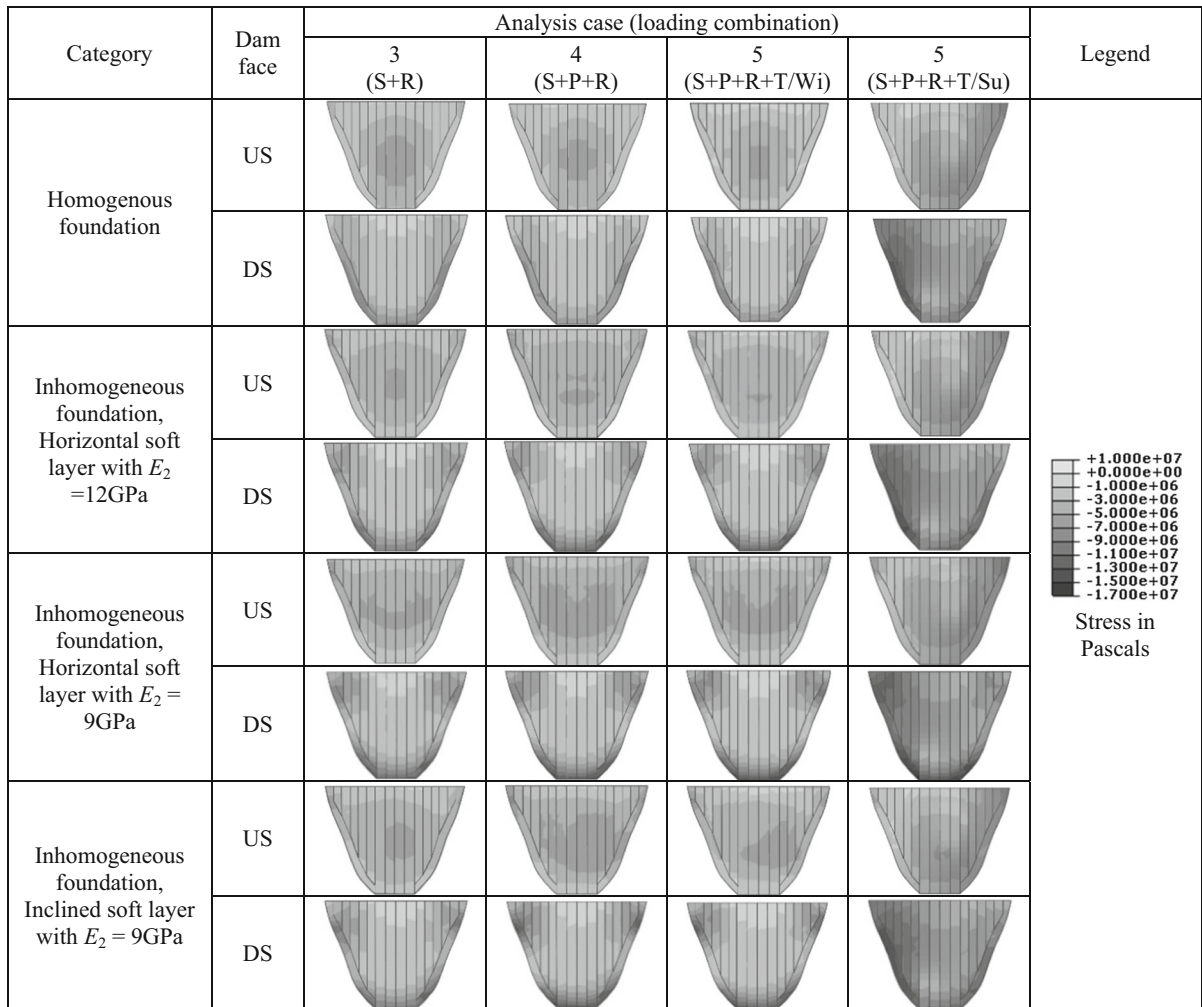


Fig. 10 Envelope contours of principal compressive stress on the upstream (US) and downstream (DS) faces of the dam for the cases 3, 4 and 5 during the operation phase

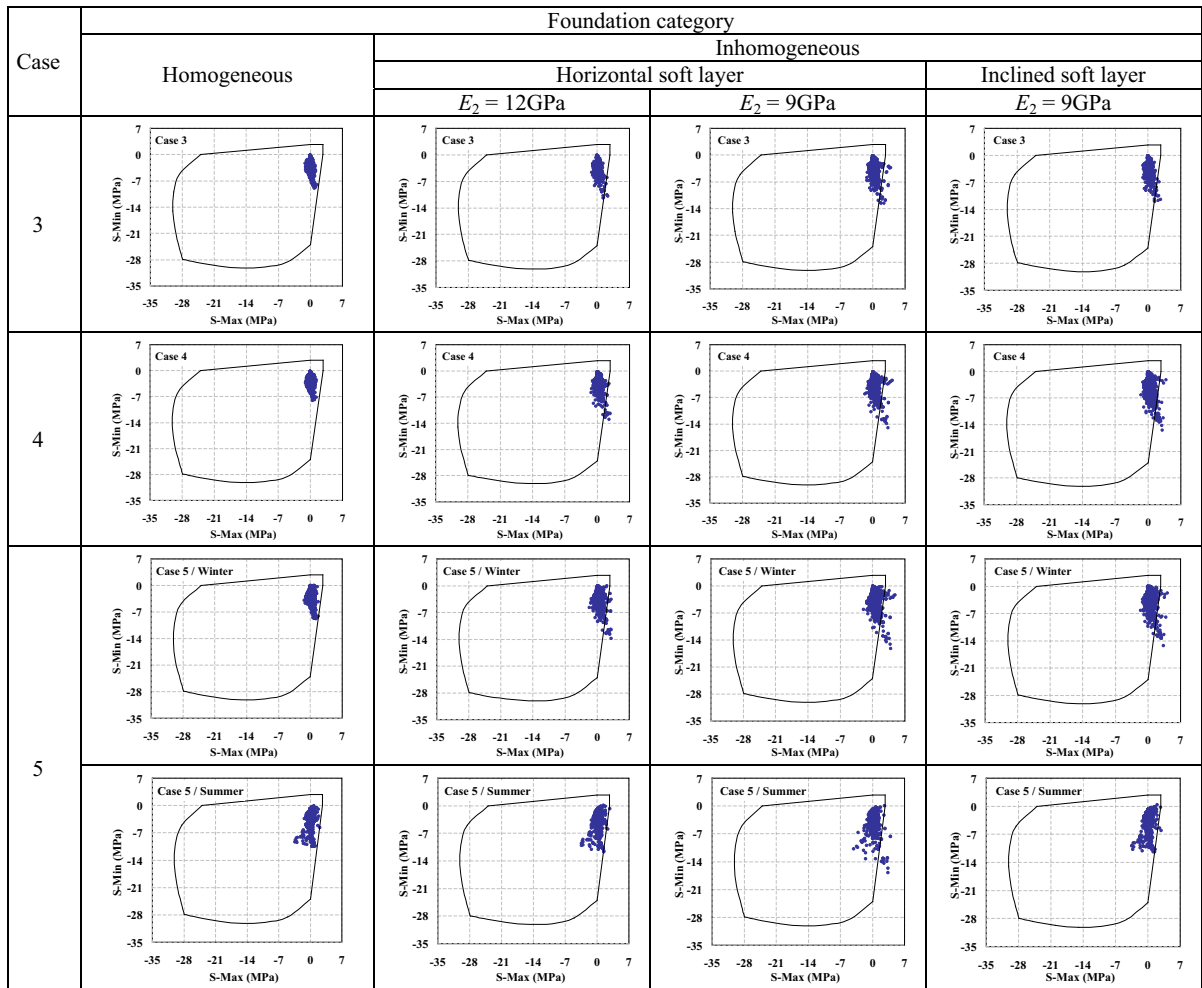


Fig. 11 Biaxial stress state of the dam body during the operation phase versus the biaxial failure curve, S-Min, minimum principal stress; S-Max, maximum principal stress

is generated using the modified relationships represented by Kupfer et al. (1969). As it is observed, in the homogeneous foundation category the stress state of the dam body satisfy the biaxial failure criteria. However, in the inhomogeneous foundation category, some nodes fall beyond the failure curve specifically for the models with softer layer. These points are generally located at the dam-foundation interface near soft rock layer. Comparing the cases 3 and 4 shows that the post-cooling causes more nodes to fall beyond the failure curve. In addition, the stress state is more critical in the winter than the summer conditions.

The peak principal stresses of the foundation in the operation phase of all cases are listed in Table 6. The stresses are marginally changed through various cases.

The joints reduce the peak tensile while increase the peak compressive stresses. The post-cooling decreases the peak principal stresses in the homogenous foundation; it would be vice versa for the inhomogeneous foundations. The homogenous foundation, opposed to the inhomogeneous foundations, experiences more stress in the summer than the winter conditions. The horizontal soft rock layer decreases the peak tensile stress in the foundation with respect to the homogeneous foundation; however the softer layer causes more stress. But the inclined soft rock layer generally increases the peak tensile stress of the foundation. The peak tensile stress is 2.336 MPa, and the peak compressive stress is -4.608 MPa for the foundation with inclined soft layer during the winter. These

Table 6 Peak principal stress, in MPa, in the foundation during the operation phase

Case	Load combination	Foundation category							
		Homogeneous		Inhomogeneous					
		S-Max	S-Min	Horizontal soft layer				Inclined soft layer	
				$E_2 = 12$ GPa		$E_2 = 9$ GPa		$E_2 = 9$ GPa	
S-Max	S-Min			S-Max	S-Min	S-Max	S-Min		
1	S + R	1.827	- 3.592	1.036	- 3.584	1.132	- 3.578	1.514	- 3.675
2	S + R	1.328	- 3.908	0.579	- 3.608	0.788	- 3.641	1.026	- 3.656
3	S + R	1.160	- 3.597	0.643	- 3.603	0.810	- 3.650	1.677	- 3.713
4	S + P+R	0.937	- 3.364	0.767	- 3.653	0.837	- 3.686	1.950	- 3.798
5	S + P+R + T/Wi	1.100	- 3.576	0.877	- 3.667	0.915	- 3.707	2.336	- 4.608
	S + P+R + T/Su	1.193	- 3.903	0.679	- 3.589	0.800	- 3.675	1.464	- 3.682

S-Min, minimum principal stress; S-Max, maximum principal stress

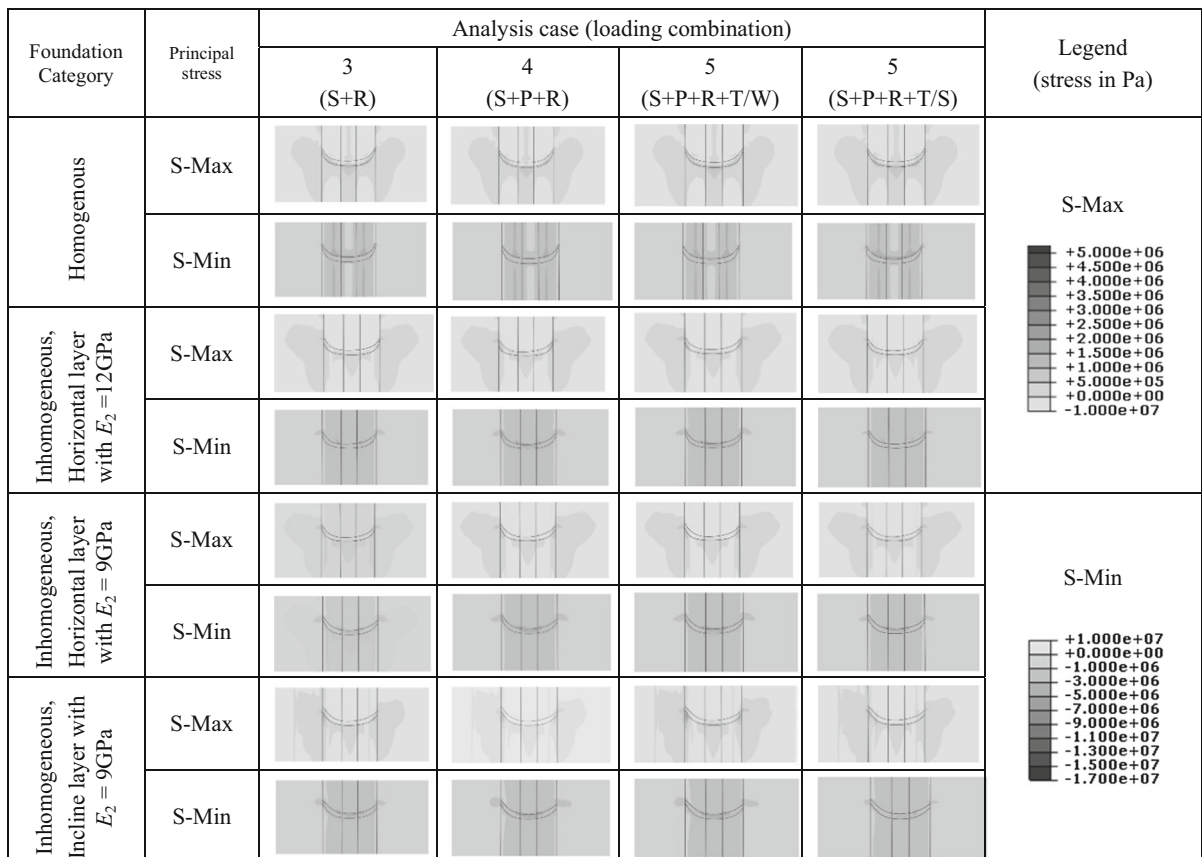


Fig. 12 Envelope contours of principal stresses in the foundation rock for the cases 3–5 in the operation phase from above view. S-Min, minimum principal stress, S-Max, maximum principal stress

stresses are within the typical rock’s compressive and tensile strength ranges. The envelope contours of principal stresses of the foundation in the vicinity of dam structure during the operation phase are depicted in Fig. 12. For the homogeneous foundation, the peak stresses are observed at the canyon bottom, but in the inhomogeneous foundation, the peak tensile stresses are observed near the soft rock layers. The contours are generally the same; however, un-symmetric contours are observed for the case of inclined soft rock layer.

4.2 Joints Safety Evaluation

The joints play key role in dam safety evaluation specifically during the operation phase. The contours of joints opening during the operation phase for the cases 2–5 are displayed in Fig. 13. In this figure, the black color represents the closed state. The peripheral joint is opened in the intermediate and lower levels from the US face. Its opening is minor in the bottom of canyon for the homogenous foundation category. The presence of the soft rock layer increases its opening at the lower and intermediate levels. The softer layer causes more opening. The post-cooling increases this


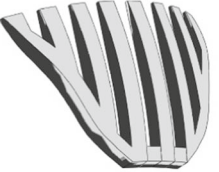


















Case	Load combination	Foundation category			
		Homogeneous	Inhomogeneous		
			Horizontal soft layer		Inclined soft layer
			$E_2 = 12\text{GPa}$	$E_2 = 9\text{GPa}$	
2	S+R				
3	S+R				
4	S+P+R				
5	S+P+R+T/W				
	S+P+R+T/S				

Fig. 13 Contours of joints opening during the operation phase of the cases 2–5; black color represents the closed state

opening; it is more in the winter than the summer condition. About the contraction joints, in general, the foundation condition has minor effect on their openings which are observed just at the upper dam levels. The largest opening belongs to the middle joint from the DS face; it may be totally opened at the crest level in the cases 4 and 5. However, some opening could occur from the US face for the side joints. The stage-construction partially increases the opening of contraction joints, but the post-cooling has no considerable effect. Again, the winter condition causes more opening than the summer condition.

The relative sliding displacements of the various contraction joints at the crest (dam elevation = 142 m) and an intermediate level (dam

elevation = 79 m) of the cases 3–5 during the operation phase are shown in Fig. 14. The plots are symmetric about the middle joint in which the relative displacement is zero, except for the cases with inclined soft rock layer. As it is expected, more sliding is observed for the crest than the intermediate level. The relative sliding at the crest and intermediate levels is generally lower than 2.5 and 1.0 mm, respectively; it increases by approaching to the abutment however it suddenly decreases for the last side joints. The sliding displacements are generally close together between various cases, but softer rock layer causes more sliding displacement. For the crest level, the minimum sliding belongs to the case 3. The relative sliding for the homogeneous and inhomogeneous foundation with

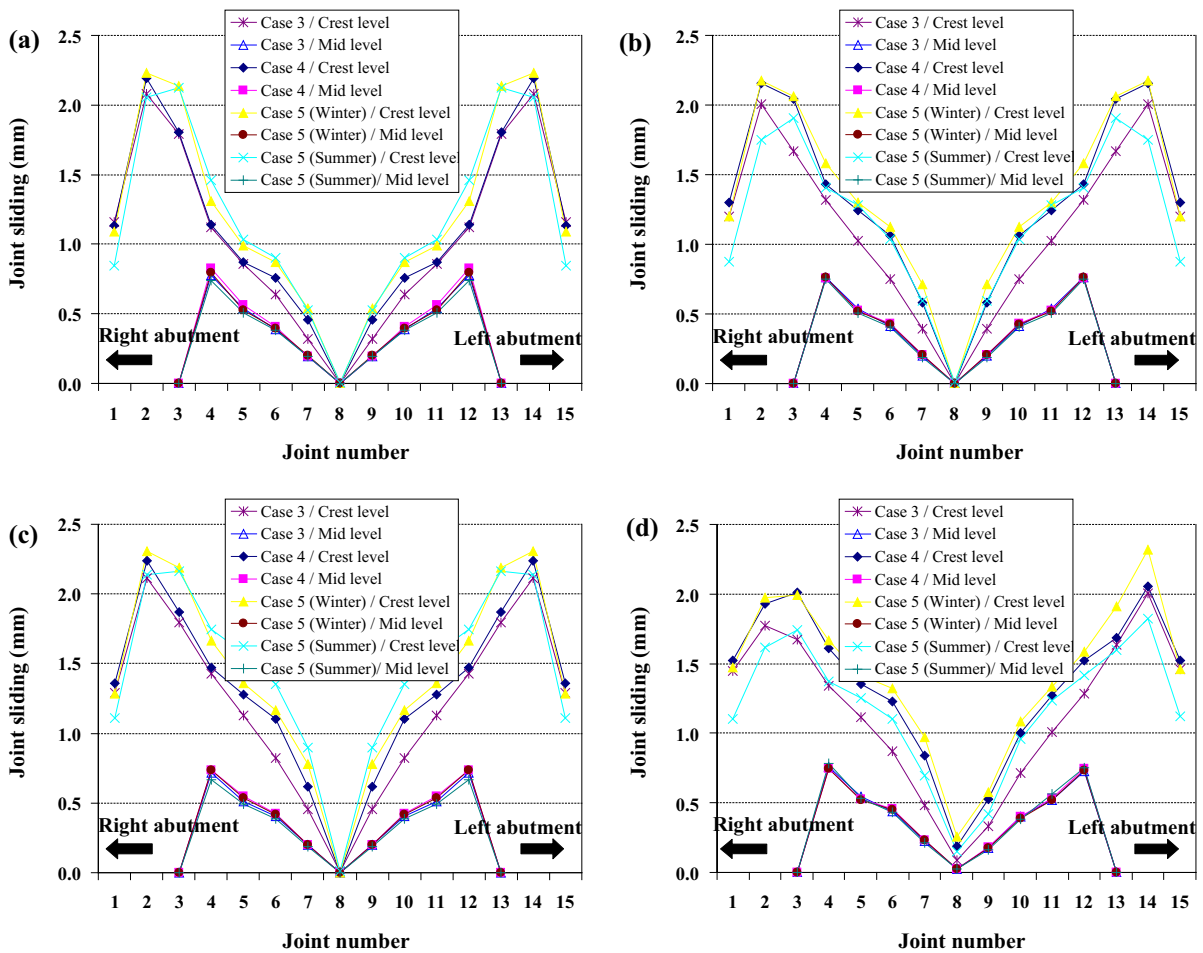


Fig. 14 Relative joints sliding displacements in the operation phase of the cases 3–5, at the crest and an intermediate level. **a** Homogeneous foundation. **b** Inhomogeneous foundation, horizontal soft rock layer with $E_2 = 12$ GPa. **c** Inhomogeneous

foundation, horizontal soft rock layer with $E_2 = 9$ GPa. **d** Inhomogeneous foundation, inclined soft rock layer with $E_2 = 9$ GPa

softer horizontal layer is more in the summer than the winter, and vice versa for the rest of the models. The inclined soft rock layer causes more sliding near the left than the right.

4.3 Displacement Results

The relative displacement of the monoliths no. 9 and 13 (Fig. 4a) under the operating loading combinations are shown in Fig. 15. As it is expected, the center cantilever, i.e. the monolith no. 9, has more relative displacement with respect to the side cantilever. The case 1 has the lowest displacement specifically for the lower levels for both monoliths. The joints increase the relative displacements specifically for the inhomogeneous foundation category. The difference between various cases is minor for the homogenous foundation category. The largest relative displacements are generally observed during the winter condition. The most values of displacement belong

to the case 5 in the winter condition. Considering the stage construction process increases the relative displacements but the post-cooling decreases them. The softer rock layer causes more displacements, but they are lowered by inclination of the soft layer. The dispersion of the results is more for the center cantilever than the side cantilever.

5 Concluding Remarks

A computational methodology is proposed for the safety evaluation of the arch dams during the construction and operation phases. It includes foundation modeling, stage-construction process, thermal post-cooling analysis, realistic behavior of contraction and peripheral joints, reservoir filling, and operational thermal loading. The methodology is applied to a typical arch dam-foundation system. The foundation is assumed to be homogenous and inhomogeneous by

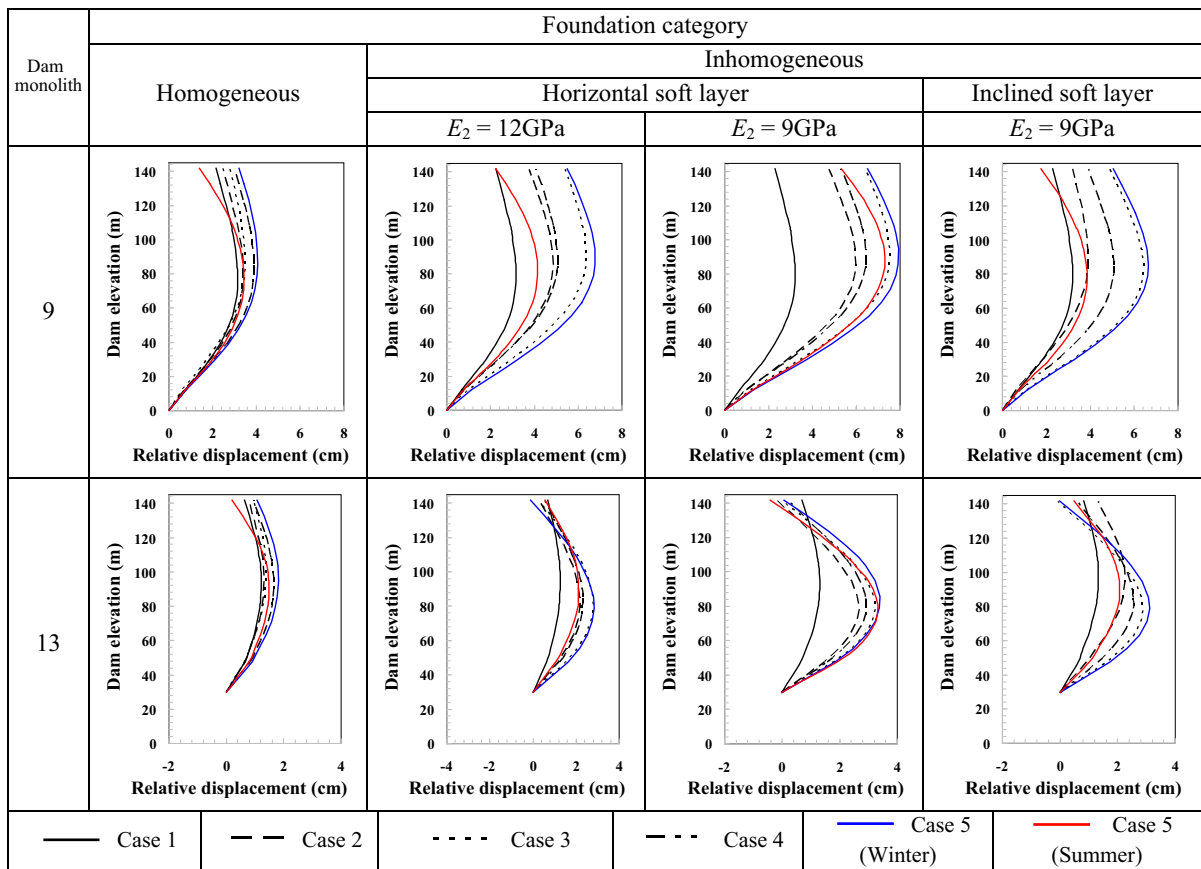


Fig. 15 Comparison of relative displacement of two monoliths no. 9 and 13, under the operating loading combination of various cases

inserting soft rock layers within it. The soft rock layer is horizontal and inclined according to typical conditions of dam-sites. The dam-foundation system is three-dimensionally modeled using finite element method and its structural safety is assessed using safety indices through some analysis cases. The results show that the dam generally has no problem in compression during the construction and operation phases under its most prominent static loads. The soft rock layer in conjunction with the post-cooling thermal loading can significantly increase the tensile stress values within the dam body during the construction phase. The presence of the joints releases the tensile stresses but increases the peak compressive stress of the dam body. Therefore, they generally help the dam anti-cracking safety. Considering the stage-construction process decreases the peak tensile stress during the construction phase, however it increases the tensile and compressive stresses during the operation phase. The post-cooling thermal loading increases both tensile and compressive stresses in construction and operation phases, specifically for the inhomogeneous foundation category. So it should be considered for cracking safety of the dam body. In addition, the thermal ambient loads have significant effects for causing probable cracks in a region of the downstream face in comparison with self-weight and hydrostatic loads.

The horizontal soft rock layer increases the peak tensile and compressive stresses of the dam body; the softer layer causes more stress. However, inclined soft rock layer with respect to the related horizontal layer, generally causes lower tensile stresses specifically during the operation phase. Therefore, it is concluded that more attention should be paid to the horizontal soft rock layers of the foundation. The inclined soft rock layer increases the compressive stress during the construction phase, but generally decreases it during the operation phase. The presence of the soft rock layer causes inhomogeneous displacement of the dam body and changes the tensile and compressive stress distribution within the dam body. The tensile stress is more on the downstream face and concentrated near the bottom of soft rock layer. The peak compressive stress is often concentrated at the bottom of the dam on the downstream face. The biaxial stress evaluation of the dam body shows that the inhomogeneity of the foundation and the post-cooling causes more critical stress state of the dam body. In addition, the stress state

is more critical in the winter than the summer conditions.

In the rock foundation, the stresses are marginally changed through various cases. The joints reduce the peak tensile while increase the peak compressive stresses. The post-cooling decreases the peak principal stresses in the homogenous foundation; it would be vice versa for the inhomogeneous foundations. The homogenous foundation, opposed to the inhomogeneous foundations, experiences more stress in the summer than the winter conditions. The horizontal soft rock layer decreases the peak tensile stress in the foundation with respect to the homogenous foundation; again, the softer layer causes more stress. But the inclined soft rock layer generally increases the peak tensile stress of the foundation. For the homogeneous foundation, the peak stresses are observed at the canyon bottom, but in the inhomogeneous foundation, the peak tensile stresses are observed near the soft rock layers.

The peripheral joint is opened in the intermediate and lower levels from the US face. The presence of the soft rock layer increases its opening at the lower and intermediate levels. The softer layer causes more opening. The post-cooling increases this opening; it is more in the winter than the summer condition. About the contraction joints, in general, the foundation condition has minor effect on their openings which are observed just at the upper dam levels. The softer rock layer causes more sliding displacement of the contraction joints. Finally, it should be noted that the obtained results are limited to the case studies investigated in this paper. The conditions may be different for other case studies.

References

- Alonso EE, Pinyol NM, Pineda J (2014) Foundation of a gravity dam on layered soft rock: shear strength of bedding planes in laboratory and large “in situ” tests. *Geotech Geol Eng* 32(6):1439–1450
- Azmi M, Paultre P (2002) Three-dimensional analysis of concrete dams including contraction joint non-linearity. *Eng Struct* 24(6):757–771
- Bayraktar A, Altunışık AC, Sevim B, Kartal ME, Türker T, Bilici Y (2009) Comparison of near and far fault ground motion effects on the nonlinear response of dam-reservoir-foundation systems. *Nonlinear Dyn* 58(4):655–673

- Bofang Z (1997) Prediction of water temperature in deep reservoir. *Dam Engineering* 8(1):13–25
- Chen S-h, Qiang S, Shahrour I, Egger P (2008) Composite element analysis of gravity dam on a complicated rock foundation. *Int J Geomech* 8(5):275–284
- Chen Y, Zhang L, Yang G, Dong J, Chen J (2012) Anti-sliding stability of a gravity dam on complicated foundation with multiple structural planes. *Int J Rock Mech Min Sci* 55:151–156
- Cook RD (2007) *Concepts and applications of finite element analysis*. Wiley, New York
- Du X, Jin T (2007) Nonlinear seismic response analysis of arch dam-foundation systems-part II opening and closing contact joints. *Bull Earthq Eng* 5(1):121–133
- Du X, Zhang Y, Zhang B (2007) Nonlinear seismic response analysis of arch dam-foundation systems-part I dam-foundation rock interaction. *Bull Earthq Eng* 5(1):105–119
- Federal Energy Regulatory Commission (1999) *Engineering guidelines for the evaluation of hydropower projects*. Chapter 11-Arch Dams. Washington DC 20426:11–18
- Florin T (2013) The freeze–thaw cycles and deterioration of concrete to hydraulic structures: the daniel johnson dam case study. *J Appl Eng Sci* 3(2):105–108
- Gaspar A, Lopez-Caballero F, Modaresi-Farahmand-Razavi A, Gomes-Correia A (2014) Methodology for a probabilistic analysis of an RCC gravity dam construction. Modelling of temperature, hydration degree and ageing degree fields. *Eng Struct* 65:99–110
- Hosseinzadeh A, Nobarinasab M, Soroush A, Lotfi V (2013) Coupled stress–seepage analysis of Karun III concrete arch dam. *Proc Inst Civ Eng Geotech Eng* 166(5):483–501
- Jaafar MS, Bayagoob KH, Noorzaei J, Thanoon WA (2007) Development of finite element computer code for thermal analysis of roller compacted concrete dams. *Adv Eng Softw* 38(11):886–895
- Joshi SG, Gupta ID, Murnal PB (2015) Analyzing the effect of foundation inhomogeneity on the seismic response of gravity dams. *Int J Civ Struct Eng* 6(1):11
- Kupfer H, Hilsdorf HK, Rusch H (1969) Behavior of concrete under biaxial stresses. *Int J Proc* 66(8):656–666
- Leger P, Venturelli J, Bhattacharjee SS (1993) Seasonal temperature and stress distributions in concrete gravity dams. Part 1: modelling. *Can J Civ Eng* 20(6):999–1017
- Lin G, Jianguo D, Zhiqiang H (2007) Earthquake analysis of arch and gravity dams including the effects of foundation inhomogeneity. *Front Archit Civ Eng China* 1(1):41–50
- Lombardi G (1991) Kölnbrein dam: an unusual solution for an unusual problem. *Int Water Power Dam Constr* 43(6):31–34
- Noorzaei J, Bayagoob KH, Thanoon WA, Jaafar MS (2006) Thermal and stress analysis of Kinta RCC dam. *Eng Struct* 28(13):1795–1802
- Oberhuber P. 2015. Karun IV arch dam, abnormal behavior and rehabilitation. Mahab Ghods Consulting Engineers
- Pausz S, Nowotny H, Jung G (2016) Rock mass classification and geotechnical model for the foundation of a RCC gravity dam. *Geomech Tunn* 8(5):436–440
- Polivka RM, Wilson EL (1976) Finite element analysis of nonlinear heat transfer problems. Report no. UCB/SESM-76/2, Department of Civil Engineering, University of California, Berkeley
- Pourbakhshian S, Ghaemian M (2015) Investigating stage construction in high concrete arch dams. *Indian J Sci Technol* 8(14):69510
- Sevim B, Bayraktar A, Altunışık AC (2011a) Finite element model calibration of berke arch dam using operational modal testing. *J Vib Control* 17(7):1065–1079
- Sevim B, Bayraktar A, Altunışık AC (2011b) Investigation of water length effects on the modal behavior of a prototype arch dam using operational and analytical modal analyses. *Struct Eng Mech* 37(6):593–615
- Sevim B, Altunışık AC, Bayraktar A (2012) Experimental evaluation of crack effects on the dynamic characteristics of a prototype arch dam using ambient vibration tests. *Comput Concr* 10(3):277–294
- Sevim B, Altunışık AC, Bayraktar A (2014) Construction stages analyses using time dependent material properties of concrete arch dams. *Comput Concr* 14(5):599–612
- Sheibany F, Ghaemian M (2006) Effects of environmental action on thermal stress analysis of Karaj concrete arch dam. *J Eng Mech* 132(5):532–544
- SNCLD (1985) *Swiss dams, monitoring and maintenance*. Swiss National Committee on Large Dams
- Takalloozadeh M, Ghaemian M (2014) Shape optimization of concrete arch dams considering abutment stability. *Sci Iran Trans A Civ Eng* 21(4):1297–1308
- Urbistondo R, Yges L (1985) Fragmentation of the El Atazar Dam foundation rock after 14 years in operation. *Proc ICOLD* 2:673–692
- USACE (1994) *Arch dam design*. Department of the Army, US Army Corps of Engineers, Engineer Manual 1110-2-2201, Washington, DC
- USBR (1997) *Level 2 thermal study mass gradient and surface gradient analysis procedure and examples*. ETL 1110-2-542, USA
- Wang W, Ding J, Wang G, Zou L, Chen S (2011) Stability analysis of the temperature cracks in Xiaowan arch dam. *Sci China Technol Sci* 54(3):547–555
- Yazdani Y, Alembagheri M (2017) Seismic vulnerability of gravity dams in near-fault areas. *Soil Dyn Earthq Eng* 102:15–24
- Zhang L, Wang D, Zhang H, Wang W (2008) Stability analysis of gravity dams on sloping layered rock foundation against deep slide. In: *Earth and space 2008: engineering, science, construction, and operations in challenging environments*, pp 1–6
- Zou D, Han H, Liu J, Yang D, Kong X (2017) Seismic failure analysis for a high concrete face rock fill dam subjected to near-fault pulse-like ground motions. *Soil Dyn Earthq Eng* 98:235–243